Analysis of Three-Dimensional Quadratic Failure Criteria for Thick Composites using the Direct Micromechanics Method

Christopher Stamblewski, Bhavani V. Sankar and Dan Zenkert

Journal of Composite Materials 2008; 42; 635
DOI: 10.1177/0021998307088609

Analysis of Three-Dimensional Quadratic Failure Criteria for Thick Composites using the Direct Micromechanics Method

CHRISTOPHER STAMBLEWSKI
Department of Aeronautical and Vehicle Engineering
Royal Institute of Technology, Stockholm, Sweden

BHAVANI V. SANKAR*
Department of Mechanical and Aerospace Engineering, PO Box 116250
University of Florida, Gainesville, FL 32611-6250, USA

DAN ZENKERT
Department of Aeronautical and Vehicle Engineering
Royal Institute of Technology, Stockholm, Sweden

ABSTRACT: Currently fiber composites are used in thick structures with significant out of plane stresses for which new 3D failure criteria are required. In this article the direct micromechanics method is used to determine the exact failure envelope of a unidirectional graphite/epoxy composite. A hexagonal unit cell of the composite is modeled using finite elements. Assuming that the failure criteria for the fiber and matrix materials and for the fiber-matrix interface are known, the exact failure envelope is constructed from a large number of three-dimensional stress states that correspond to failure initiation in the composite. These 3D failure stress states are then used to develop five three-dimensional phenomenological failure criteria: maximum stress; maximum strain; quadratic stress; quadratic strain; and optimized quadratic failure criteria. It is observed that the 3D quadratic stress and strain failure criteria may not always be closed, that is, they predict infinite strength in some directions. They can be made closed in combination with the maximum stress or the maximum strain failure criterion. It is found that a combination of aforementioned 3D failure criteria make failure prediction in thick composites more accurate and reliable. It is noted that the newly proposed optimized quadratic failure criteria is always closed, and is found to be more reliable than all other 3D failure criteria.

KEY WORDS: direct micromechanics method, failure criteria, fiber composites, finite element analysis, graphite/epoxy, micromechanics, periodic boundary conditions, unit-cell analysis.

*Author to whom correspondence should be addressed. E-mail: sankar@ufl.edu
Figures 2 and 4–9 appear in color online: http://jcm.sagepub.com

0021-9983/08/07 0635–20 $10.00/0 DOI: 10.1177/0021998307088609

Los Angeles, London, New Delhi and Singapore

INTRODUCTION

CURRENT FAILURE CRITERIA for unidirectional fiber composites assume a state of plane stress and are therefore only applicable to thin laminates. With improved manufacturing technology, fiber composites are used in thicker structures with significant out of plane stresses, for which the plane stress assumption is no longer valid and thus, 2D failure criteria are no longer reliable. Therefore, a new criterion, which does not assume a state of plane stress, is needed for thick composites. In this paper, several 3D failure criteria are proposed and their efficacies are evaluated.

To analyze the accuracy and reliability of a failure criterion, the failure envelope predicted by that criterion is compared with the actual failure envelope of the composite. The actual failure envelope can be developed from either experimental measurements or numerical simulations. In this article, the actual failure stresses were obtained using the direct micromechanics method (DMM), which is a finite element based micromechanical failure analysis of the unit cell of the composite.

Fiber composites have been successfully analyzed using micromechanical methods in the past, but most often to determine thermo-mechanical properties [1–4] and not for strength predictions. Lin et al. [5] performed a finite element micromechanical analysis of fiber composites to determine the elastic-plastic behavior under uni-axial loading, while the effects of thermal residual stresses on the strength were analyzed by Ishikawa [6]. Strength prediction under multi-axial loading conditions is not practical and hence phenomenological failure criteria are still used in the industry instead of micromechanical models. The most common phenomenological 2D failure criteria are the maximum stress criterion, the maximum strain criterion and quadratic interaction criteria, such as the Tsai–Hill and the Tsai–Wu failure criteria [7].

The DMM was initially proposed by Sankar and was demonstrated in several papers, e.g., Zhu et al. [8], Marrey and Sankar [9] and (Karkkainen and Sankar) [10–12]. In Zhu et al. [8] the DMM failure envelopes were compared with the phenomenological failure criteria for plane stress states. It was observed that a combination of the maximum stress and the Tsai–Wu criteria is the best choice for predicting the failure for thin unidirectional fiber composites. A similar observation, based on experimental results, was made by Daniel and Ishai [11], as it was recommended that one should use several failure criteria and choose the most conservative criterion for a given state of stress. Karkkainen and Sankar [10] analyzed failure initiation of plain weave textile composites with DMM, where a failure envelope for in-plane force resultants – with and without applied bending moment resultants – was developed and compared with phenomenological failure criteria.

In this article, several 3D failure criteria are proposed and their accuracy and reliability are evaluated. It is assumed that the failure stress states predicted by the DMM constitute the actual or real failure envelope, and we compare the proposed phenomenological criteria against the DMM failure envelope. A particular failure criterion is evaluated by studying how often the criterion predicts conservatively and how large the average difference compared to the DMM failure stresses is. Ideally, a closed failure criterion, which never predicts infinite strength and with no difference compared to the DMM, is desired. For the finite element analysis in this study, a hexagonal unit cell is chosen as described by Li [12] and as implemented by Choi and Sankar [13].

Initially, four 3D phenomenological failure criteria based on the DMM results are proposed: (i) maximum stress theory; (ii) maximum strain theory; (iii) 3D quadratic stress theory; and (iv) 3D quadratic strain theory. The quadratic failure criteria are similar to the

Tsai–Wu failure criterion, but they do not assume a state of plane stress and consider all six stresses. A similar criterion was developed for thin textile composite plates by Karkkainen et al. [14], but considering three forces and three moments, instead of the six stresses. The strength coefficients for the proposed phenomenological criteria are obtained from uni-axial and bi-axial failure states determined from the DMM.

Obviously the maximum stress and strain theories are closed, meaning they always yield closed failure envelopes. However, there is no guarantee that the failure envelopes of 3D quadratic theories derived from uni-axial strength values will be closed. That is, they may predict infinite strength in some directions. In order to ensure a closed envelope, a new quadratic theory called optimized quadratic failure theory is proposed. The strength coefficients of this theory are optimized with respect to random DMM failure stress states and not from the uni-and bi-axial failure stresses as in conventional quadratic failure theories.

DIRECT MICROMECHANICS METHOD

In the present study, the failure stresses and the failure envelope are obtained using the DMM, which is a finite element based micromechanical analysis of the composite unit cell. The finite element analysis is performed for six linearly independent unit strains. Then, by proper superposition, the microstress field can be determined for any given homogenous macrostress state in the composite. Failure stresses for the composite can be determined when failure criteria for the constituent elements are defined. The failure macrostresses that are obtained from the micromechanical failure analysis in DMM are assumed to be the real failure stresses, and can be compared with predicted failure stresses from any other failure criterion to check how accurate and reliable it is.

The DMM is essentially used as an analytical laboratory that successfully simulates physical testing of the composite. It can overcome the limitations of physical equipment and can quickly determine diverse and complex failure stress states that include 3D stress states. Of course, any failure criterion should be verified by performing various strength tests on actual composite specimens before being used in design.

Finite Element Analysis

The objective of the finite element analysis is to determine the stress distribution in the unit cell for six linearly independent deformations for further analysis in DMM. Six strain cases are analyzed, where in each case, the unit cell is subjected to one of the unit strains ε_1, ε_2, ε_3, γ_{23}, γ_{13} or γ_{12}, while the others strains are set to zero.

For the present study, graphite/epoxy composite, a common aerospace material, is chosen. The material properties for the transversely isotropic graphite fiber are presented in Table 1, while the material properties for the isotropic epoxy matrix are given in Table 2. The fiber and matrix properties were obtained form references [13] and [15], respectively.

A hexagonal unit cell with a fiber volume fraction of 60% is analyzed in this article. A hexagonal unit cell is chosen, as it is closer to random fiber distribution compared to a square unit cell. The side length of the hexagon is taken as 10 μm, the fiber radius is 4.07 μm and the unit cell thickness is 0.2 μm. It should be mentioned that the actual dimensions of the unit cell does not matter, and the fiber volume fraction is the key parameter. The hexagonal unit cell is presented in Figure 1 with its coordinate system and

Table 1. Graphite fiber properties.

E_{f1} (GPa)	E_{f2}, E_{f3} (GPa)	G_{f12}, G_{f13}, G_{f23} (GPa)	ν_{f12}, ν_{f13}	ν_{f23}
263	19	27.6	0.2	0.35

Table 2. Epoxy matrix properties.

E_m (GPa)	G_m (GPa)	ν_m
3.2	1.19	0.35

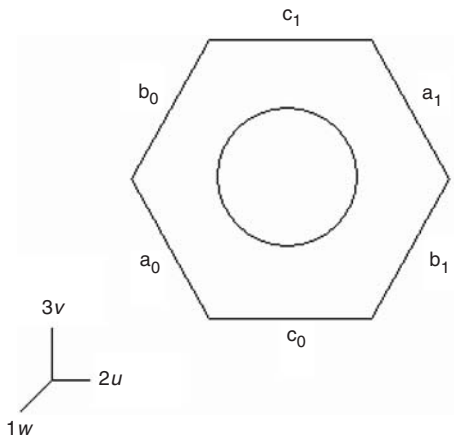

Figure 1. *Unit cell surfaces and the coordinate system definitions.*

surface definitions. The cross section surface of the hexagonal unit cell is modeled with more than 4500 elements for high accuracy, while in the thickness direction only two elements are used to reduce the total number of elements and hence the computational time. In fact, the present analysis can be performed using generalized plane strain elements, as the stresses are uniform in the 1-direction. However, 3D elements are used to facilitate implementation of periodic boundary conditions on faces normal to the 1-direction.

To maintain compatibility of the displacements and continuity of the stress distribution between each unit cell, each boundary of a unit cell has to deform as the adjoining boundary of the adjacent unit cell. These constraints are enforced with periodic boundary conditions, which are presented in Table 3 for the six different strain cases.

The deformations and the stress distributions for the six strain cases as obtained from the finite element analysis are illustrated in Figure 2.

Homogenized Material Properties

From the finite element analyses of the six linearly independent unit strains, the stiffness matrix $\boldsymbol{C}$, that relates the macrostrains ε with the macrostresses σ, according to

$$\sigma = C\varepsilon \tag{1}$$

Table 3. Periodic boundary conditions for the hexagonal unit cell for six different unit strains.

$\varepsilon_1 = 1$	$\varepsilon_2 = 1$	$\varepsilon_3 = 1$	$\gamma_{23} = 1$	$\gamma_{13} = 1$	$\gamma_{12} = 1$
$u_{a1}-u_{a0}=0$	$u_{a1}-u_{a0}=\sqrt{3}/2L$	$u_{a1}-u_{a0}=0$	$u_{a1}-u_{a0}=0$	$v_{z1}-v_{z0}=0$	$u_{z1}-u_{z0}=0$
$u_{b1}-u_{b0}=0$	$u_{b1}-u_{b0}=\sqrt{3}/2L$	$u_{b1}-u_{b0}=0$	$u_{b1}-u_{b0}=0$	$w_{c1}=L/2$	$u_{c1}=0$
$v_{a1}-v_{a0}=0$	$v_{a1}-v_{a0}=0$	$v_{a1}-v_{a0}=L/2$	$u_{c1}=0$	$w_{c0}=-L/2$	$u_{c0}=0$
$v_{b1}-v_{b0}=0$	$v_{b1}-v_{b0}=0$	$v_{b1}-v_{b0}=-L/2$	$u_{c0}=0$	$w_{a1}-w_{a0}=L/2$	$v_{c1}=0$
$v_{c1}=0$	$v_{c1}=0$	$v_{c1}=L/2$	$v_{a1}-v_{a0}=\sqrt{3}/2L$	$w_{b0}-w_{b1}=L/2$	$v_{c0}=0$
$v_{c0}=0$	$v_{c0}=0$	$v_{c0}=-L/2$	$v_{b1}-v_{b0}=\sqrt{3}/2L$		$w_{a1}-w_{a0}=\sqrt{3}/2L$
$w_{z1}-w_{z0}=t$	$w_{z1}-w_{z0}=0$	$w_{z1}-w_{z0}=0$	$w_{z1}-w_{z0}=0$		$w_{b1}-w_{b0}=\sqrt{3}/2L$

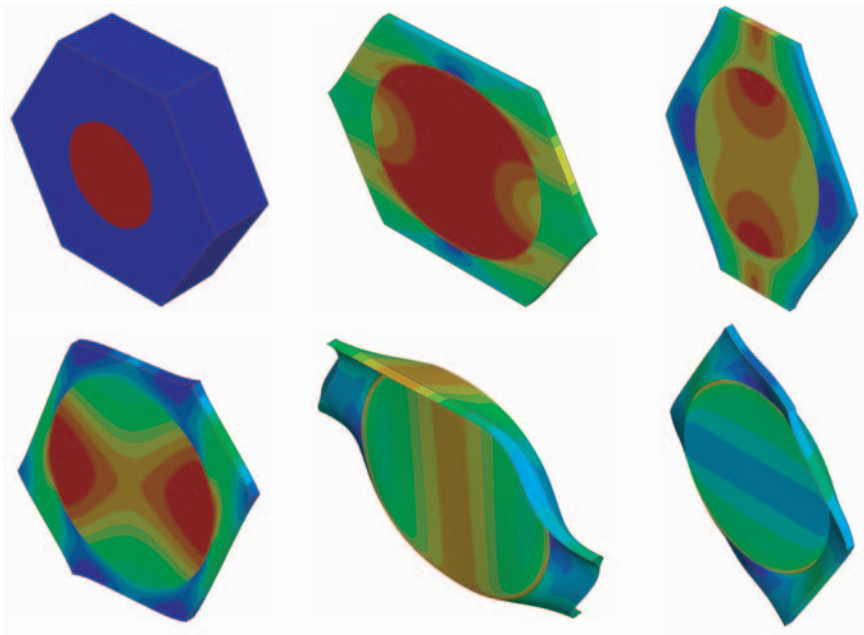

Figure 2. *The deformed shape of the unit cell for various strain cases: (a) ε_1, (b) ε_2, (c) ε_3, (d) γ_{23}, (e) γ_{13}, and (f) γ_{12}.*

can be determined. With the stiffness matrix, the elastic constants of the composite can be obtained using the relation

$$C^{-1} = \begin{bmatrix} 1/E_1 & -\nu_{21}/E_2 & -\nu_{31}/E_3 & 0 & 0 & 0 \\ -\nu_{12}/E_1 & 1/E_2 & -\nu_{32}/E_3 & 0 & 0 & 0 \\ -\nu_{13}/E_1 & -\nu_{23}/E_2 & 1/E_3 & 0 & 0 & 0 \\ 0 & 0 & 0 & 1/G_{23} & 0 & 0 \\ 0 & 0 & 0 & 0 & 1/G_{31} & 0 \\ 0 & 0 & 0 & 0 & 0 & 1/G_{12} \end{bmatrix}. \tag{2}$$

If the macrostresses and the macrostrains for each unit strain case are related as in Equation (1), then it can be seen that the elastic constants C_{ij} in the column corresponding

to the unit strain are equal to the macrostresses. For example, the elastic constant C_{11} is equal to the resulting σ_1 from the strain case $\varepsilon_1 = 1$. The six macrostresses σ_i for each unit strain case are calculated as the volume average of the corresponding microstresses $\sigma_i^{(e)}$ in NEL elements according to

$$\sigma_i = \frac{1}{V}\sum_{e=1}^{NEL} \sigma_i^{(e)} V^{(e)}, \quad i = 1 \ldots 6, \tag{3}$$

where $\sigma_i^{(e)}$ are the stresses at the centroid of element e, $V^{(e)}$ is the volume of element e and V is the total volume of the unit cell. For the graphite/epoxy composite in the present example, the stiffness matrix is obtained as

$$C = \begin{bmatrix} 161.0 & 3.8 & 3.8 & 0 & 0 & 0 \\ & 10.4 & 4.6 & 0 & 0 & 0 \\ & & 10.4 & 0 & 0 & 0 \\ & & & 3.9 & 0 & 0 \\ & SYM & & & 3.6 & 0 \\ & & & & & 3.3 \end{bmatrix} \text{GPa}. \tag{4}$$

To make sure that there are no major mistakes in the finite element model, the calculated material properties are compared with material properties obtained with Halpin-Tsai semi-empirical relations [15] as shown in Table 4. It should be noted that the Halpin-Tsai equations are empirical in nature, which could explain the difference in G_{12} and G_{13}.

Micromechanical Failure Analysis

With the results from the finite element analysis and with the calculated stiffness matrix, the microstress distribution within the unit cell can be analyzed for any given macrostress state. In the present study, the unit cell is analyzed for tensile and compressive failure in all matrix and fiber elements, as well as for fiber/matrix interface tensile/shear failure. It is assumed that the combined composite has failed if only one of the fiber or matrix elements or if one of the fiber-matrix interface nodes has failed. This is a conservative assumption

Table 4. Material properties of graphite/epoxy composite. Elastic constants are in GPa.

	DMM Results	Halpin-Tsai equations
E_1	159.1	159.08
E_2, E_3	8.3	8.496
G_{12}	3.3	4.1
G_{13}	3.6	4.1
G_{23}	3.9	–
ν_{12}, ν_{13}	0.253	0.26
ν_{23}	0.436	–

but can be considered as the initiation of failure. For the fiber and the matrix, the maximum principal stress criterion is used, while for the interface, maximum tensile stress and maximum interfacial shear stress criteria are used. In Table 5, the failure stresses for the graphite fiber and the epoxy matrix as well as for the interface are presented [15]. Further, fiber microbuckling is also investigated as it is assumed that the hexagonal unit cell fails if the fiber buckles. However, it is observed that fiber microbuckling is never critical for the analyzed graphite/epoxy as the calculated fiber stress at microbuckling is higher than the critical fiber compressive stress.

For any given macrostress state σ_0, the corresponding macrostrains

$$\varepsilon_0 = C^{-1}\sigma_0 \tag{5}$$

are used to determine the microstresses in each of the finite element and at the fiber/matrix interface nodes by superposition of the six unit macrostrain cases from the finite element analysis. With the appropriate failure criterion, a load factor λ^e for each element and interface node is determined, where the load factor is defined as the factor by which the given macrostresses have to be increased to initiate failure in element e. The load factor that initiates failure in the composite is the minimum of all element load factors, and it is denoted by λ_{DMM}. The corresponding failure stress state is then given by

$$\hat{\sigma}_{\mathrm{DMM}} = \lambda_{\mathrm{DMM}}\sigma_0. \tag{6}$$

In the present study, about 5000 random stress states σ_0 are generated, where both positive and negative stresses have equal probability in all directions to obtain diverse failure stress states. The flow chart of the micromechanical failure analysis is presented in Figure 3.

PHENOMENOLOGICAL FAILURE CRITERIA

A smooth surface in the 6-dimensional space that passes through all the generated failure stress states could be considered as the DMM failure envelop of the composite. Although DMM can be used in practice to check if a given stress state is within or outside the envelope, it is not convenient in the design of composite structures. A phenomenological criterion in terms of the six components of stresses is desirable in design, especially in using structural optimization methods. Hence, the use of DMM results in generating several phenomenological failure criteria for thick composites is investigated and their accuracy is evaluated by comparing with the DMM failure envelope. The phenomenological criteria consider in the present study are: (i) maximum stress theory, (ii) maximum strain theory; (iii) 3D quadratic stress failure criterion; and (iv) 3D quadratic strain failure criterion. For reasons that will be given later, a new optimized 3D quadratic failure criterion is also developed.

Table 5. The failure stresses for the graphite and epoxy materials and the graphite/epoxy interface.

Failure stress (MPa)	Graphite	Epoxy	Interface
Tension, σ_{Tcr}	4,120	49	127
Compression, σ_{Ccr}	2,990	121	–
Shear, τ_{cr}	1,760	93	243

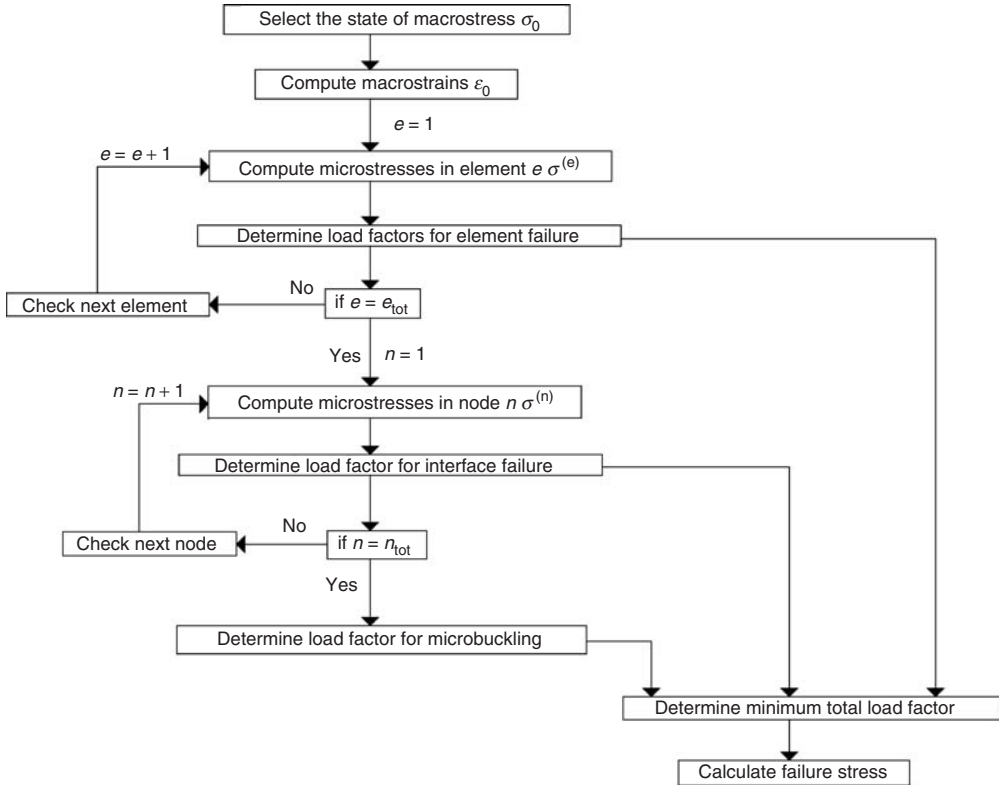

Figure 3. *The flow chart of the micromechanical failure analysis.*

Maximum Stress Theory

The failure envelope according to the maximum stress theory, which we will denote by $M\sigma$, is a rectangular solid in the six-dimensional space similar to a rectangle in 2D or a rectangular parallelepiped in 3D stress space. The maximum stress theory is given by

$$-S_{iC} \leq \sigma_i \leq S_{iT}, \quad i = 1, 2, 3 \tag{7}$$

and

$$|\sigma_i| \leq S_i, \quad i = 4, 5, 6 \tag{8}$$

where the various uni-axial strengths of the composites, S_{iC} and S_{iT}, and shear strengths S_{i} can be determined using DMM. The symbols $S_{i\mathrm{T}}$ and $S_{i\mathrm{C}}$ denote the tensile and compressive strengths, respectively.

Maximum Strain Theory

Similar to the maximum stress theory, the maximum strain theory, $M\varepsilon$, is given by

$$-R_{iC} \leq \varepsilon_i \leq R_{iT}, \quad i = 1, 2, 3 \tag{9}$$

and

$$|\varepsilon_i| \leq R_i, \quad i = 4, 5, 6 \tag{10}$$

Again, the uni-axial failure strains $R_{i\mathrm{C}}$ (compression) and $R_{i\mathrm{T}}$ (tension) and maximum shear strains R_i can be determined using the DMM.

3D Quadratic Stress Failure Criterion

A 3D quadratic stress failure criterion, DQ^{σ}, is proposed, where failure will occur if

$$\sum\sum E_{ij}\bar{\sigma}_i\bar{\sigma}_j + \sum F_i\bar{\sigma}_i > 1 \tag{11}$$

where

$$\bar{\sigma}_i = \frac{\sigma_i}{S_{iT}} \ (i = 1, 2, 3), \quad \bar{\sigma}_i = \frac{\sigma_i}{S_i} \ (i = 4, 5, 6) \tag{12}$$

is the stress component σ_{i} normalized with respect to corresponding tensile strength $S_{i\mathrm{T}}$ or shear strength S_i. The stresses are normalized due to the great disparity in the magnitude of the strength values, which otherwise could lead to numerically ill-conditioned calculations.

The procedures for determining the coefficients E_{ij} and F_i are similar to that for 2D quadratic failure criterion [16]. The coefficients E_{ij} and F_i in (11) are obtained assuming they satisfy all the uni-axial and bi-axial failure states determined by the DMM. With uni-axial tensile failure stress states, (11) is simplified as

$$E_{ii} + F_i = 1 \quad (i = 1, 3; \text{no summation over repeated indices}) \tag{13}$$

while with uni-axial compressive failure stresses it is simplified as

$$E_{ii}\left(\frac{S_{iC}}{s_{iT}}\right)^2 - F_i\left(\frac{S_{iC}}{S_{iT}}\right) = 1. \tag{14}$$

For the case of shear, the uniaxial tensile and compressive states will be replaced by positive and negative shear stress states. Solving (13) and (14) simultaneously, the coefficients E_{ii} and F_i in the failure equation (11) are obtained. The off-diagonal elements E_{ij} are obtained from the bi-axial failure stress states such that

$$\bar{\sigma}_i = \bar{\sigma}_j. \tag{15}$$

In that case, (11) can be reformulated as

$$E_{ij} = \frac{1}{2\bar{\sigma}_i\bar{\sigma}_j}\left(1 - E_{ii}\bar{\sigma}_i^2 - E_{jj}\bar{\sigma}_j^2 - F_i\bar{\sigma}_i - F_j\bar{\sigma}_j\right), \quad i \neq j \tag{16}$$

The uni-axial and bi-axial failure stresses obtained from the DMM and are presented in Tables 6 and 7.

Table 6. Uniaxial Strengths obtained using the DMM. The strength values are in MPa.

S_{1T}	S_{1C}	S_{2T}	S_{2C}	S_{3T}	S_{3C}	S_4	S_5	S_6
2,312	1,809	39.2	97.2	31.1	73.4	24.0	31.9	33.2

Table 7. Biaxial strength values in MPa units obtained using the DMM.

Failure stress	σ_1	σ_2	σ_3	τ_{23}	τ_{13}	τ_{12}
σ_1	–	39.3	31.1	24.0	31.7	33.0
σ_2		–	43.5	16.4	26.7	20.1
σ_3			–	20.5	18.1	24.6
τ_{23}				–	19.9	16.5
τ_{13}					–	21.7
τ_{12}						–

From the DMM failure stresses presented in Tables 6 and 7, the coefficients E and F in the 3D quadratic failure criterion ($3DQ^{\sigma}$) are obtained as

$$E = \begin{bmatrix} 1.2782 & 0.1213 & 0.0957 & -0.0552 & 0.5933 & 0.4883 \\ & 0.4040 & -0.5780 & 0.3773 & -0.2558 & 0.2527 \\ & & 0.4230 & -0.2626 & 0.3005 & -0.2288 \\ & & & 1 & -0.0793 & 0.4122 \\ & SYM & & & 1 & 0.1242 \\ & & & & & 1 \end{bmatrix} \tag{17}$$

and

$$F = \begin{pmatrix} -0.2782 & 0.5960 & 0.5770 & 0 & 0 & 0 \end{pmatrix}^T. \tag{18}$$

3D Quadratic Strain Failure Criterion

A 3D quadratic strain failure criterion, $3DQ^{\varepsilon}$, is also proposed, where failure occurs if

$$\sum\sum \tilde{E}_{ij}\varepsilon_i\varepsilon_j + \sum \tilde{F}_i\varepsilon_i > 1. \tag{19}$$

The method of determining the failure coefficients $\tilde{E}_{ij}$ and $\tilde{F}_i$ is similar to that of $3DQ^{\sigma}$, but with uni-axial and bi-axial failure strains. Observe that the criterion (19) does not have to be normalized as in (11), because there is no big disparity in the magnitude of failure strains as in the case of strength values. With failure strains from the DMM,

Table 8. Eigenvalues of the coefficient matrix E of the 3D Quadratic Stress criterion.

−0.19	0.29	0.45	0.71	1.85	1.99

the coefficients are obtained as

$$\tilde{E} = \begin{bmatrix} 10405 & 8121 & 10714 & 7299 & 8216 & 6630 \\ & 29901 & -23008 & 21795 & 2275 & 7283 \\ & & 42685 & -7777 & 8251 & -3874 \\ & & & 27141 & -957 & 6438 \\ & SYM & & & 12511 & 1147 \\ & & & & & 10045 \end{bmatrix} \tag{20}$$

and

$$\tilde{F} = \begin{pmatrix} 29.08 & 123.81 & 142.59 & 0 & 0 & 0 \end{pmatrix}^T. \tag{21}$$

Combined Criterion

For any failure criterion to be physically possible it must have a closed surface, that is, it should not predict infinite strength in any direction or for any given ratio of stresses. The maximum stress and maximum strain criteria are closed as they are represented by a rectangular solid in the 6D space. However, the quadratic failure criteria, derived from uni-axial and bi-axial strength values, may not be always closed. It can be shown that the requirement for a closed quadric surface given by (11) is that the matrix $\boldsymbol{E}$ must be positive definite, which implies that all the eigenvalues of $\boldsymbol{E}$ must be positive. For the example considered here with the coefficient matrix given in (17), the quadratic failure criterion is not closed as the matrix is not positive definite as seen from the eigen values presented in Table 8.

It is observed that the $3DQ^{\sigma}$ criterion predicts infinite failure stresses five times out of the 5000 randomly generated 3D stress states. Similarly, the $3DQ^{\varepsilon}$ sometimes predicts infinite failure stresses as the matrix $\tilde{E}$ is not positive definite either. This phenomenon is illustrated in Figure 4, where the failure envelopes for the $3DQ^{\sigma}$, maximum stress (Mσ) and maximum strain (Mε) criteria in the σ_2-σ_3 space ($\sigma_1 = \tau_{12} = \tau_{13} = \tau_{23} = 0$) are presented together with 250 random DMM failure stresses. As it can be seen, the quadratic criterion is not closed in this space.

Hence, the quadratic failure criteria are not recommended to be used by themselves as they might predict infinite failure stresses. They should therefore always be considered in combination with other closed failure criteria. In this paper, they are combined with both $M\sigma$ and $M\varepsilon$. Three combined criteria are proposed; $3DQ^{\sigma}/M\sigma/M\varepsilon$, $3DQ^{\varepsilon}/M\sigma/M\varepsilon$ and a combination of both quadratic failure criteria, $3DQ^{\sigma}/3DQ^{\varepsilon}/M\sigma/M\varepsilon$.

Similarly, Figure 5 depicts the failure criteria in the σ_1-σ_2 space ($\sigma_3 = \tau_{12} = \tau_{13} = \tau_{23} = 0$). One can note that a combination of the three individual phenomenological criteria yields conservative results when compared to DMM envelope.

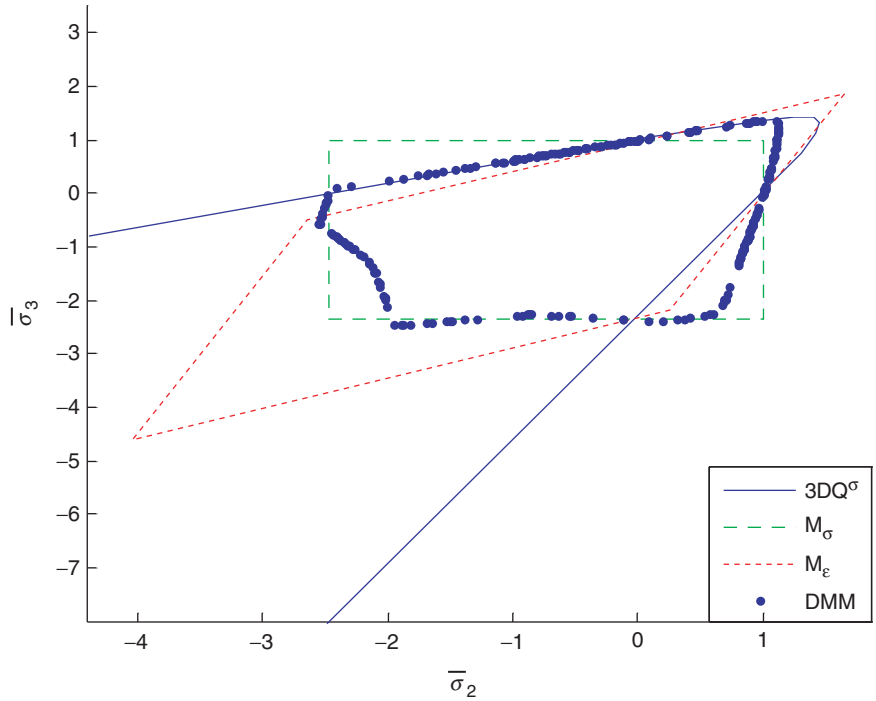

Figure 4. *Failure envelopes in the σ_2-σ_3 space for the 3DQ$^\sigma$, Mσ and Mε criteria. Also shown is the envelope of 250 random DMM failure stresses.*

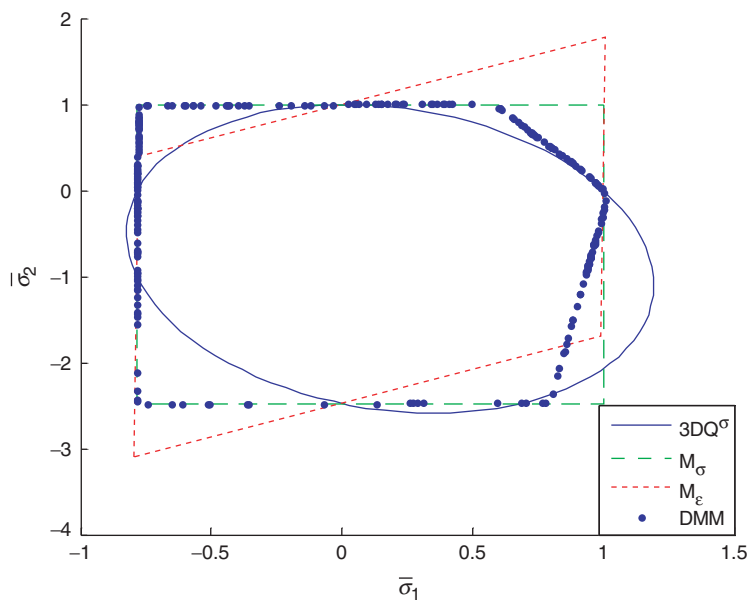

Figure 5. *Failure envelopes in the σ_1-σ_2 space for the 3DQ$^\sigma$, Mσ and Mε failure criteria. Also shown is the envelope of 250 random DMM failure stresses.*

Criteria Comparison

We would also like to know the effects of using 2D failure criteria when the stress state is truly three-dimensional. This we accomplish by including the Tsai–Wu criterion to the list of phenomenological criteria to be evaluated. The 2D and 3D failure criteria are compared with the 5000 randomly generated DMM failure stresses. The average difference between the analyzed criterion and DMM for M number of stress states is given by,

$$\bar{\delta} = \frac{\sum_{m=1}^{M} \delta_m}{M} \tag{22}$$

where

$$\delta_m = 1 - \frac{\lambda_m}{\lambda_{\mathrm{DMM}}} \tag{23}$$

is the difference between the load factors for a particular criterion and the DMM for the mth stress state. With this definition, a positive difference implies a conservative result, where the failure criterion predicts a lower failure stress than the DMM.

The standard deviation ϕ and the root mean square difference ψ are also determined for the failure criteria as a measure of accuracy according to

$$\phi = \sqrt{\frac{1}{M}\sum_{m=1}^{M}\left(\delta_m - \bar{\delta}\right)^2} \tag{24}$$

and

$$\psi = \sqrt{\frac{\sum_{m=1}^{M} \delta_m^2}{M}} \tag{25}$$

The reliability of a particular failure criterion is determined by the percentage of conservative results.

In Table 9, the accuracy and reliability for complex 3D stress states for various criteria are compared, where the average difference, standard deviation, the root mean square

Table 9. The accuracy and reliability of different criteria for random 3D stress states.

Criterion	Average difference [%]	Standard deviation [%]	Root mean square diff [%]	Conservative results [%]
$M\sigma$	−50	41	65	10
$M\varepsilon$	−423	48	64	20
2DQ	−61	82	102	15
Mσ/Mε	−40	44	59	22
2DQ/Mσ/Mε	−26	37	45	28
3DQ$^{\sigma}$/Mσ/Mε	−1.8	28	28	56
3DQ$^{\varepsilon}$/Mσ/Mε	−0.33	35	35	59
3DQ$^{\sigma}$/3DQ$^{\varepsilon}$/Mσ/Mε	5.3	28	29	65

Table 10. The accuracy and reliability of maximum stress, maximum strain and 2D quadratic failure criteria for pure 2D stress states.

Criterion	Average difference [%]	Standard deviation [%]	Root mean square diff [%]	Conservative results [%]
$M\sigma$	−4.9	9.3	10	32
$M\varepsilon$	−3.6	20	21	34
$2DQ$	2.1	15	15	65

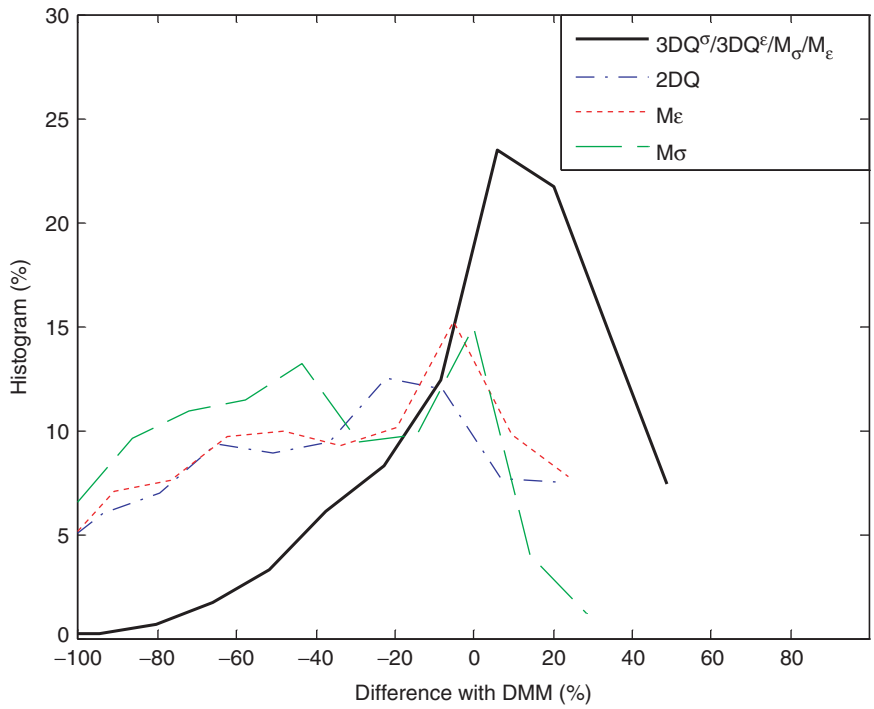

Figure 6. *Histogram comparison of various failure criteria compared with 5000 DMM failure stress states. Positive difference with respect to the DMM failure stress denotes conservative result.*

difference and the percent of conservative results are presented. Further, for the 2D criteria, the accuracy and the reliability for pure 2D stress states are presented in Table 10. As it is observed, for complex 3D cases, the quadratic criteria (in combination with $M\sigma$ and $M\varepsilon$) are more reliable and accurate than the 2D criteria. Further, the accuracy and reliability of the combined $3DQ^{\sigma}/3DQ^{\varepsilon}/M\sigma/M\varepsilon$ for complex 3D stress states, as seen in Table 9, is comparable with the accuracy and reliability of the $3DQ$ for thin fiber composites with pure 2D stress states, as seen in Table 10.

Finally, a histogram comparison between the combined $3DQ^{\sigma}/3DQ^{\varepsilon}/M\sigma/M\varepsilon$ criteria and the 2D criteria for a set of random 3D DMM failure stresses is presented in Figure 6. As mentioned earlier, a positive difference implies a conservative result, while a negative difference implies that failure stress is over predicted compared with the DMM

failure stresses. One can see that the reliability determined by the percentage of conservative predictions is very high for the combined criterion.

OPTIMIZATION OF FAILURE CRITERIA

As mentioned earlier, the quadratic criteria are not always completely closed, as in some cases the coefficient matrices can have negative eigenvalues. Thus, the quadratic criteria have to be combined with the other closed failure criteria. Further, as the coefficients for the quadratic criteria are determined with the uni-axial and the bi-axial failure states, it is assumed that only these measurements are completely true, as the criterion is fitted to these values. This is a reasonable assumption when experimental measurements are used, because these are usually the only failure states that can be measured. However, if the DMM is used, it is possible to obtain more complex failure states, which should be, just as the uni-axial and bi-axial failure states, equally true.

Therefore, it is investigated if it is possible to fit a criterion to more diverse DMM failure stresses and if a more reliable and accurate criterion can be obtained. Also, it is analyzed if it is possible to obtain a quadratic failure criterion that is closed by itself.

Optimized Quadratic Failure Criterion

In this section, the development of an Optimized 3D quadratic failure criterion (OQFC), which is closed and also satisfies a given number of DMM failure states, is described. In the optimization, the volume of a closed 6D ellipsoid is maximized for a given failure states, i.e., the 6D ellipsoid should be as big as possible within the given failure states. For a closed ellipsoid, the eigenvalues of the matrix $\boldsymbol{E}$ should be positive. However, it is known that the volume of the ellipsoid is inversely proportional to the product of its eigenvalues, which is equal to the determinant of the matrix $\boldsymbol{E}$. Thus, the problem can be stated as an optimization problem in which the coefficients $\boldsymbol{E}^{\text{opt}}$ and $\boldsymbol{F}^{\text{opt}}$ are selected such that

$$\begin{aligned} &\text{Minimize: } f(E_{ij}^{\text{opt}}, F_i^{\text{opt}}) = \det\left[2E^{\text{opt}}\right] \\ &\text{Subjected to the constraints: } \sum\sum E_{ij}^{\text{opt}} \bar{\sigma}_i^{(k)} \bar{\sigma}_j^{(k)} + \sum F_i^{\text{opt}} \bar{\sigma}_i^{(k)} > 1, \quad k = 1 \ldots N \\ &\text{eigenvalues of } E^{\text{opt}} > 0 \end{aligned} \tag{26}$$

where N is the number of DMM failure stress states selected for the optimization problem. Further, to ensure that the positive and the negative shear strengths are equal, the condition

$$F_4^{\text{opt}} = F_5^{\text{opt}} = F_6^{\text{opt}} = 0 \tag{27}$$

is imposed. It is also required that $\boldsymbol{E}^{\text{opt}}$ be symmetric. Thus 24 coefficients are optimized.

The MATLAB® optimizer *fmincon* was used for the optimization problem stated in (26). Although all the available DMM failure states can be used for optimization, i.e. $N = 5000$, it is found that the computational time becomes prohibitively large as N approached a few dozen states. Hence, a smaller number compared to 5000 for N is used in the

present analysis. However, the accuracy and the reliability of the optimized quadratic failure criterion are still evaluated by comparing with the all of the DMM failure states.

Optimization with DMM Failure Stresses

The accuracy and the reliability of the OQFC depend on how many DMM failure stress states N are used for the optimization process. In Figure 7(a), the percentage of conservative results is plotted against the number N. One can note that the reliability of OQFC reaches about 90% with $N = 30$ failure states used in the optimization. Thereafter, the convergence is slow in the sense that one may need a large N to improve the reliability.

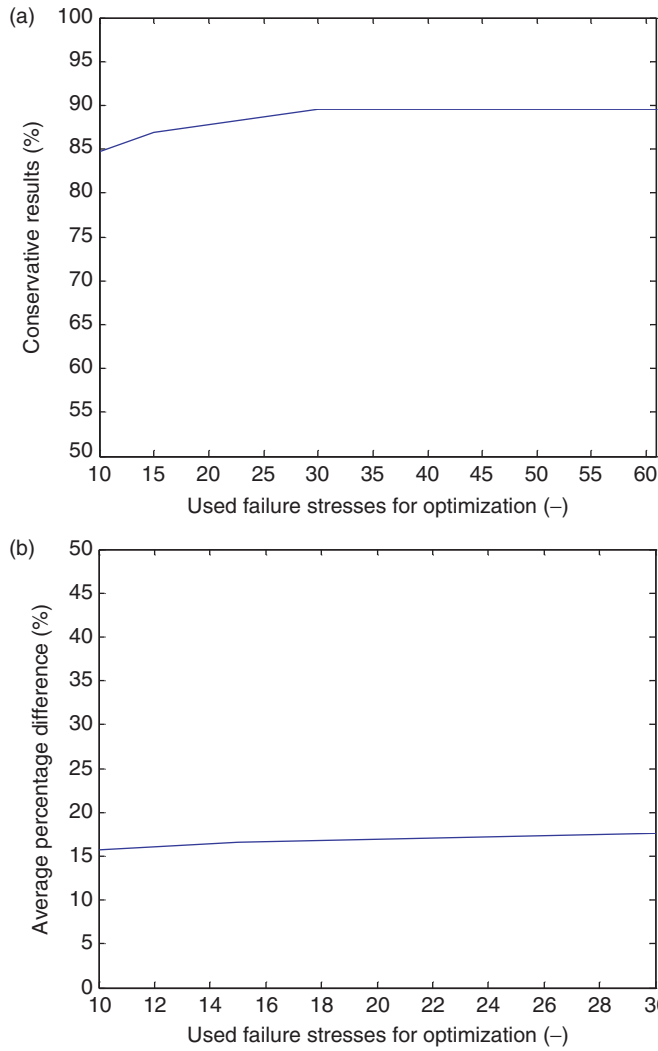

Figure 7. *(a) Conservative results and (b) average difference as functions of number of failure stresses used in the optimization.*

At this time the computational resources do not seem to be adequate for this purpose. The average difference between OQFC and DMM are plotted against N in Figure 7(b).

For the purpose of illustration the optimized coefficients were obtained from 30 DMM failure states (N=30) as

$$E^{\text{opt}} = \begin{bmatrix} 1.6274 & 0.1849 & 0.3909 & 0.2096 & 0.1532 & 0.1914 \\ & 0.8155 & -0.6031 & 0.3589 & -0.1911 & -0.0688 \\ & & 0.8368 & 0.0763 & -0.0773 & -0.2230 \\ & & & 1.4598 & -0.2406 & 0.1871 \\ & SYM & & & 1.5519 & 0.0207 \\ & & & & & 1.4982 \end{bmatrix} \tag{28}$$

and

$$F^{\text{opt}} = \begin{pmatrix} -0.0395 & 0.8245 & 0.6623 & 0 & 0 & 0 \end{pmatrix}^T. \tag{29}$$

Note that the coefficients are normalized with respect to uni-axial DMM tensile strength values. With these coefficients, 90% conservative results and an average percentage error of less than 18% are obtained. The uni-axial and bi-axial strength values based on the OQFC can be obtained from the coefficients given in (28) and (29). The strength values based on the OQFC are presented in Tables 11 and 12 together with the original strength values obtained from DMM.

For all optimized failure criteria, it was observed that $\boldsymbol{E}^{opt}$ has no negative eigenvalues, as this was imposed as a constraint. Thus, the optimized criterion is a closed one and does not need to be combined with other criteria to make it closed.

For the purpose of easy visualization the OQFC is compared with DMM and $3DQ^{\sigma}$ criteria in Figures 8 and 9. Figure 8 presents the failure envelopes in the non-dimensional σ_2-σ_3 space and Figure 9 corresponds to σ_1-σ_2 space.

Table 11. Optimized uni-axial failure stresses of the composite.

Strength (MPa)	S_{1T}	S_{1C}	S_{2T}	S_{2C}	S_{3T}	S_{3C}	S_4	S_5	S_6
OQFC	1841	1785	27.9	67.6	23.8	48.4	19.8	25.6	27.1
DMM	2312	1809	39.2	97.2	31.1	73.4	24	31.9	33.2

Table 12. Optimized bi-axial failure stresses of the composite. The DMM values are given in parentheses.

Failure stress (MPa)	σ_1	σ_2	σ_3	τ_{23}	τ_{13}	τ_{12}
σ_1	–	27.9 (39.3)	23.7 (31.1)	19.8 (24.0)	25.6 (31.7)	27.1 (33.0)
σ_2		–	19.8 (43.5)	13.6 (16.4)	18.7 (26.7)	18.5 (20.1)
σ_3			–	13.9 (20.5)	16.9 (18.1)	18.4 (24.6)
τ_{23}				–	17.1 (19.9)	15.1 (16.5)
τ_{13}					–	18.5 (21.7)
τ_{12}						–

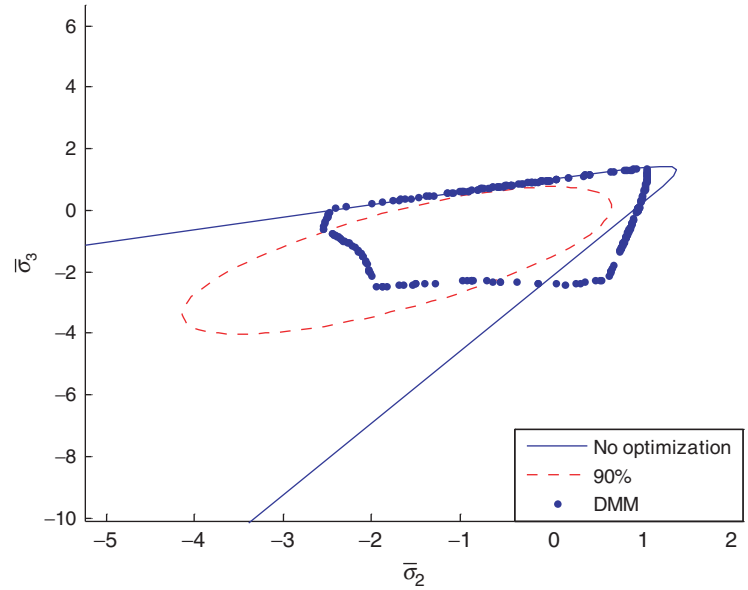

Figure 8. *2D failure envelopes in the σ_2-σ_3-space for the optimized and original quadratic failure criteria and 250 random DMM failure stresses.*

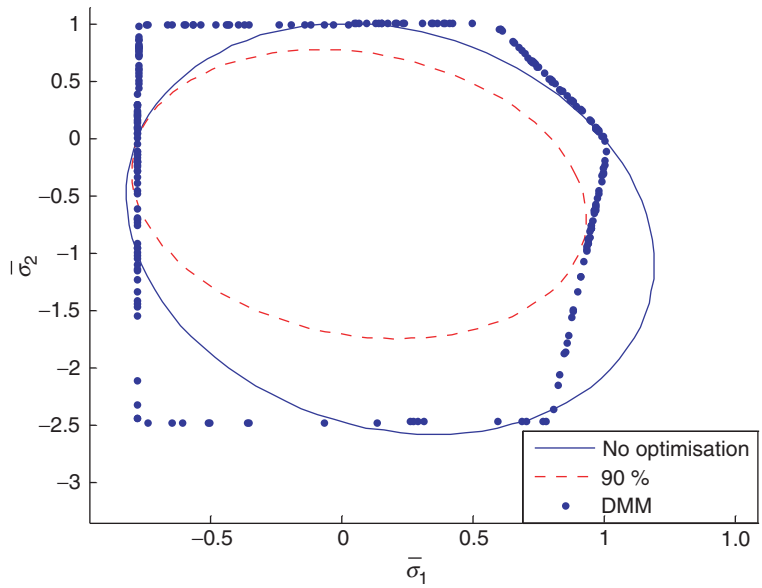

Figure 9. *2D failure envelopes in the σ_1-σ_2-space for the optimized and original quadratic failure criteria and 250 random DMM failure stresses.*

CONCLUSIONS

The DMM is used to determine a large number of random failure states of a unidirectional graphite/epoxy composite. Assuming these failure stresses represent the true failure states of the material, four 3D phenomenological failure criteria are developed. They are: maximum stress; maximum strain; quadratic stress; and quadratic strain failure criteria. It is found none of the above criteria are reliable and accurate in the entire 6D stress space. Furthermore, the quadratic stress and strain criteria may not be closed, predicting infinite strength in some directions in the 6D stress space. Instead of using the uniaxial and biaxial strength values to determine the coefficients in the quadratic failure criteria, an optimization procedure is then used to develop a 6D ellipsoid that will cover a maximum number of failure states. This criterion is called the OQFC. Some of the comparisons between various criteria are as follows.

From the analysis of the phenomenological failure criteria, it was observed that these criteria are not good for complex 3D stress states. Even if all are combined, only 27% conservative results are obtained with an average error of almost 26% over prediction of the DMM failure stresses. If they are considered separately, even worse comparison with DMM failure stresses are obtained. Thus, these criteria cannot be considered reliable and should not be used when analyzing thick fiber composites with complex 3D stress states.

If both quadratic failure criteria are combined with the maximum stress and the maximum strain failure criteria, which have closed failure envelopes, the combined criteria predicts 65% conservative results with an average difference of 5% under prediction with respect to the DMM failure stresses. This is comparable with the accuracy and reliability of 2DQ, the Tsai–Wu failure criterion, for thin fiber composites with pure 2D stress states.

From further analysis, it is observed that applying a factor of safety to the failure criteria has basically the same effect as the optimization. With a factor of safety of 1.6, the combined $3DQ^{\sigma}/M\sigma/M\varepsilon$ yielded 90% conservative results, which is as much as it is obtained with the optimized criterion, when 30 stress states are used for the optimization. However, the optimized criterion is more accurate with an average error of less than 18%, compared to the 30% error with the factor of safety approach. Thus, it could be argued that introducing a factor of safety would be an easier method to correct the original failure criterion. However, if a factor of safety is applied, the final failure criterion will have the same shape as the original criterion, i.e. a non-closed failure criterion will remain non-closed even if a factor of safety is introduced. Therefore, the quadratic failure criteria have to still be combined with other closed failure criteria, even with a factor of safety. This is easier than optimizing, but on the other hand, if optimization is used to improve the failure criterion, it is possible to enforce constraints so that the final failure criterion is closed.

In conclusion, it could be said that if only experimental methods are used to determine the failure stresses and with only uni-axial and bi-axial measurements available, the best method to create a reliable criterion is to combine the quadratic failure criteria with the maximum stress, the maximum strain or both, and applying a factor of safety so that the desired level of conservative failure envelope is obtained. However, if the failure stresses are obtained from the DMM, then an optimization of the failure criterion is recommended, as it is possible to create a more reliable, closed failure criterion, which considers more diverse failure stresses and does not necessarily have to be combined with other failure criteria. Also, as mentioned, the optimized failure criterion is more accurate than introducing a factor of safety.

ACKNOWLEDGEMENTS

The financial aid by Professor Rune Lindgren of the Royal Institute of Technology at Stockholm, Sweden is gratefully acknowledged by CS. BVS acknowledges the support of Army Research Office contract DAAD19-02-1-0330 with Dr. Bruce LaMattina as the Grant Monitor

REFERENCES

1. Dasgupta, A.S., Bhandarkar, S., Pecht, M. and Barkar, D. (1990). Thermoelastic Properties of Woven-Fabric Composites using Homogenization Techniques, In: *Proceedings of the American Society for Composites*, Fifth Technical Conference, Lansing, MI, pp. 1001–1010.
2. Foye, R.I. (1993). Approximating the Stress Field within the Unit Cell of a Fabric Reinforced Composite Using Replacement Elements, *NASA CR-191422*, Cleveland, OH.
3. Naik, R.A. (1994). Analysis of Woven and Braided Fabric Reinforced Composites, *NASA CR-194930*, Cleveland, OH.
4. Whitcomb, J.D. (1991). Three-Dimensional Stress Analysis of Plain Weave Composites, *Composite Materials Fatigue and Fracture* (Third Volume). ASTM STP 1110, pp. 417–438.
5. Lin, T.H., Salinas, D. and Ito, Y.M. (1972). Elastic-Plastic Analysis of Unidirectional Composites, *Journal of Composite Materials*, **6**(1): 48–60.
6. Ishikawa, T. (1982). Strength and Thermal Residual Stress of Unidirectional Composites, *Journal of Composite Materials*, **16**(1): 40–52.
7. Tsai, S.W. and Hahn, H.T. (1980). *Introduction to Composite Materials*, Technomic Publishing Co, Lancaster, PA.
8. Zhu, H. Sankar, B.V. and Marrey, R.V. (1998). Evaluation of Failure Criteria for Fiber Composites Using Finite Element Micromechanics, *Journal of Composite Materials*, **32**(8): 766–782.
9. Marrey, R.V. and Sankar, B.V. (1997). A micromechanical model for textile composite plates, *Journal of Composite Materials*, **31**(12): 1187–1213.
10. Karkkainen, R.L. and Sankar, B.V. (2006). A Direct Micromechanics Method for Analysis of Failure Initiation of Plain Weave Textile Composites, *Composites Science and Technology*, **66**(1): 137–150.
11. Daniel, I.M. and Ishai, O. (1994). *Engineering Mechanics of Composite Materials*, Oxford University Press, New York, USA.
12. Li, S. (1999). On the Unit Cell for Micromechanical Analysis of Fibre-reinforced Composites, In: *Proceedings of the Royal Society of London*, *Series A*, **455**(1983): 815–838.
13. Choi, S. and Sankar, B.V. (2006). Micromechanical Analysis of Composite Laminates at Cryogenic Temperatures, *Journal of Composite Materials*, **40**(12): 1077–1091.
14. Karkkainen, R.L., Sankar, B.V. and Tzeng, J.T. (2007). A Direct Micromechanical Approach towards the Development of Quadratic Stress Gradient Failure Criteria for Textile Composites, *Journal of Composite Materials*, **41**(16): 1917–1937.
15. Zenkert, D. and Battley, M. (2005). *Foundations of Fibre Composites*, Universitetsservice US AB, Stockholm, Sweden.
16. Hahn, H.T. and Tsai, S.W. (1980). *Introduction to Composite Materials*, p. 280, Technomic Publishing Co., Westport, Connecticut.